

GRAPHITE FURNACE ATOMIC ABSORPTION SPECTROMETRY FOR THE SELECTIVE DETECTION AND QUANTIFICATION OF NANOPARTICLES

Nanostructured Materials for Nanotechnology Applications

Author: Raúl Garde Casasnovas
Director: Martín Resano Ezcaray

Abstract

In this work, ionic gold and gold nanoparticle (AuNPs) solutions/suspensions of different sizes have been studied by means of high-resolution continuum source graphite furnace atomic absorption spectrometry (HR CS GFAAS), without any separation step or any extra technique. The application of slow atomization heating ramps and atomization temperatures of around 2200°C, in the absence of chemical modifier, allows the differentiation of ions and nanoparticles according to the signal profile. In addition, the size of AuNPs can be estimated using the time of appearance of the maximum peak height, a result of 27.7 ± 8.8 nm was found for a sample provided by NIST of a nominal value of 30 nm diameter.

The analytical evaluation gave a limit of detection of 5.5 pg ($0.55 \mu\text{g L}^{-1}$) and a linear range up to 10 ng ($1000 \mu\text{g L}^{-1}$). Also, the method was successfully validated by spiking a soft water (certified reference material KEJIM 02). Finally, the possibility of determining samples mixed with both ionic and NPs showed difficulties if quantitative information is required, but the behaviour proved to be as predicted by summing the individual signals of these species.

Contents

1. Introduction	1
2. Experimental.....	3
2.1. Instrumentation	3
2.2. Standards, samples and reagents.....	4
3. Results and Discussion	6
3.1. Au Monitoring by GFAAS. Enhancing differences between ions and NPs	6
3.2. Evaluation of parameters to characterize the NP size.....	15
3.3. Analytical performance.....	18

4. Conclusions	23
5. Bibliography	24

1. Introduction

In the last years, nanotechnology has been developed at gigantic steps for the incredible properties and applications that can be applied. In particular, metallic nanoparticles (NPs) has been used in biomedical applications,^{1,2} with gold nanoparticles as the most important representative NPs of this group. Their use in therapy diagnosis and imaging has positioned team as one of the most interesting materials for medicine in the future. The high surface-volume ratio, high stability and surface reactivity combined with the capability of entering faster into cells compared with other molecules, his photophysical properties like the surface plasmon resonance, and its ability to transform radiation into heat allows its application in detection systems and thermal therapies.³ In addition, a lot of drug delivery systems studied uses gold nanoparticles as carrier for the great properties already mentioned and an incredible amount of studies involving cancer therapies.⁴

Despite the amazing properties and promising studies, the concern about safety and biocompatibility of these materials have stimulate their evaluation. Bulk gold is considered as an inert material and their reactivity and interaction is weak, but the huge changes in their properties at the nanoscale makes it a totally different material and potentially toxic.⁵ Regulatory agencies have started studies to evaluate its possible dangers in the environment and health.^{6,7}

Many techniques are used for the characterization of nanoparticles. Electron microscopies (transmission and scanning) are probably the most popular ones, as they are able to characterize properties such as size distribution and shape of nanoparticles, to obtain images of the sample and make semi quantitative analysis. SEM also presents the problem of the sample preparation may cause a contraction of it and change their characteristics. In the case of TEM, it has the advantage of being able to couple with different analytical techniques and better spatial resolution. Overall electron microscopies are strong tools, being able to characterize nanoparticles of even 1 nm. However, the need of faster, cheaper and better quantitative analysis opens the opportunity to new approaches.⁸

UV-vis have been used over the years to characterize metal nanoparticles taking advantage of their surface plasmon resonance, which is directly related with the size and concentration of the nanoparticle.⁹

Dynamic light scattering can provide size information down to 1 nm taking advantage of the Brownian motion produced by the deflection of the incident light on the sample that can be related with the size of spherical nanoparticles by the Stokes-Einstein equation. It is a non-invasive technique and short time consuming. However it presents several drawbacks, it is difficult to master, dust particles interferes in the process of scattering, modifying its intensity and a small limitation range size (1 nm-3 µm).^{8,10}

Inductively coupled plasma mass spectrometry (ICPMS) have shown as an alternative in the last few years for its capability of quantify the smaller amount of nanoparticles and also for the appearance of two methodologies that allow the size characterization of nanoparticles.¹¹⁻¹³ First, the so called single particle mode,¹⁴⁻¹⁶ and, second, the coupling to separation techniques.^{13,17} However, complex liquids and solids implies the need of preparation steps, increasing the possibilities of lose or change the original form of the nanoparticles.

The technique evaluated in this work is high resolution continuum source graphite furnace atomic absorption spectroscopy (HR CS GFAAS). Principally, this technique was used for the quantification of the total amount of a metal (expected to be found as nanoparticles) taking advantage of its possibility of analyse complex liquids and solids directly without tedious previous steps making it a fast and direct solution.¹⁸⁻²¹ However, along the years no other application related with nanoparticles was described. The traditional methodology of work with this technique involves the optimization of the parameters in order to obtain similar signals independently of the sample and the form of the element.

However, a different approach can be followed, optimizing the same parameters in order to maximize the differences between species of the same element. Three articles written

by Gagne *et al.*²² and Feitchmeier and Leopold^{23,24} demonstrate the possibility of this technique applied to Ag⁺ and silver nanoparticles (AgNPs) in solid samples with presence of elements that tend to interact with ionic silver. However, this studies are very specific, and there is a necessity of investigate the feasibility of the technique for other nanoparticles, what is the best strategy for the optimization and what parameters are the optimal for the characterization.

The purpose of this study is to develop a simple and straightforward methodology for the characterization of gold nanoparticles compare with ionic gold in a simple liquid matrix, and then to estimate the size of the nanoparticles present in the samples.

2. Experimental

2.1. Instrumentation

All the experiments were carried out with a high-resolution continuum source atomic absorption spectrometer (ContrAA 700, Analytik Jena, Jena, Germany) equipped with a transversely heated graphite furnace atomizer. The optical system schemed in **figure 1** is composed by a xenon short-arc lamp operating in ‘hot-spot’ mode as the radiation source, a high-resolution double *échelle* monochromator, and a linear CCD array detector with 588 pixels.²⁵ 200 of them are used to measure the absorbance and the rest for internal corrections. Pyrolytic graphite tubes with platforms were used to perform the analysis and also a tube without platform for a specific experiment.

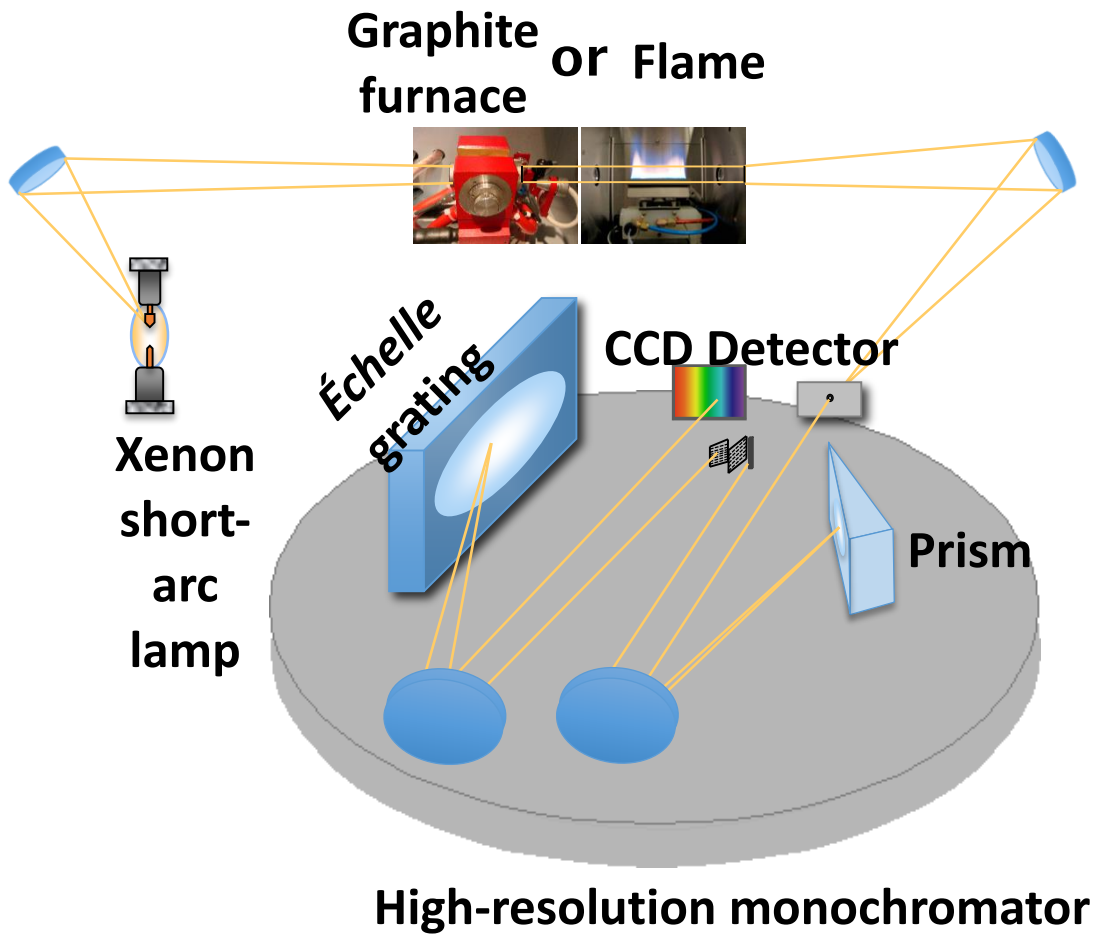


Figure 1: Optic system of the HR CS GFAAS with the radiation source, graphite furnace and flame atomizers, the two monochromators and the detection system.

2.2. Standards, samples and reagents

Purified water was obtained from a Milli-Q system (Millipore, Billerica, USA). Au ionic solutions were daily prepared by proper dilution of a 1 g L^{-1} single-element standard (Merck, Darmstadt, Germany) in HCl 0.12 M. Pd solutions were also prepared from a 1 g L^{-1} single-element standard (Merck) using purified water. H_2SO_4 diluted solutions were made from a concentrated (98%) solution (Merck). Cysteine and thiourea solutions were prepared from the respective solid reagents, diluted in HCl 0.12 M. All the reagents were of analytical grade or higher purity.

AuNPs in the form of water suspensions were acquired from Nanocomposix (Prague, Czech Republic). The particle size distribution of these suspensions was characterized by

TEM and their exact concentration was determined by ICPMS. Such information is provided by the manufacturer and is shown in **Table 1**. Additionally, another water suspension containing AuNP was purchased from the National Institute of Standards and Technology (NIST, Gaithersburg, USA): Reference Material 8012 Gold nanoparticles, nominal 30 nm diameter. The certificate of this material provides the NP size as estimated using 6 different techniques, with values ranging between 24.9 and 28.6 nm. However, perhaps the most accepted value is the one obtained *via* TEM (27.6 ± 2.1 nm).

Intended NP size / nm	Real mean NP size / nm	Standard deviation / nm	Concentration / g L ⁻¹
5	4.7	0.6	0.052
20	19.6	2.1	0.051
50	49	11.3	0.052
80	75.7	10.1	0.055
100	100.0	7.4	0.052

Table 1: Table with the information of the AuNPs provided by Nanocomposix.

These suspensions were further diluted in HCl 0.12 M to the required final content (5–1000 µg L⁻¹), prior to HR CS GFAAS monitoring. To avoid particle agglomeration, the original suspensions were sonicated for 5 minutes before their dilution, and the final working suspensions were sonicated for 5 minutes before HR CS GFAAS measurements.

For evaluating the performance of the method with an environmental sample, the certified reference material KEJIM 02, soft water from Kejimkujik Lake (lot 0914), was purchased from Environment Canada (Burlington, Canada) and spiked with the suspensions of the NPs of different sizes or with the Au ionic standard, until the intended Au concentration was reached. The same procedure regarding sonication that is described above was followed.

3. Results and Discussion

3.1. Au Monitoring by GFAAS. Enhancing differences between ions and NPs

The ionic gold signals obtained without any modifier shows two peaks, caused by the atomization mechanism of this element. The first peak is associated to the formation of microdroplets and the second to the interaction between the gold and carbon active sites present in the tube that delay the atomization process. This effect becomes more problematic while the tube ages.²⁶ The addition of a modifier such as ascorbic acid increases the affinity of gold for those carbon sites, augmenting the proportion of the second peak.²⁶

The typical modifier for gold analysis by GFAAS is Pd, the postulated mechanism describes the interaction of Pd with those active sites in carbon, and in this situation Au atoms will interact with Pd instead of carbon sites. When a certain temperature enough to vaporize the Pd is reached, the gold is released and the signal obtained is a unimodal peak reproducible and independent on the chemical form of the gold.^{18,30} In **Figure 2** two signals of gold (ionic and nanoparticles) were obtained with the addition of 10 µg of Pd, both signals are practically identical in area and shape.

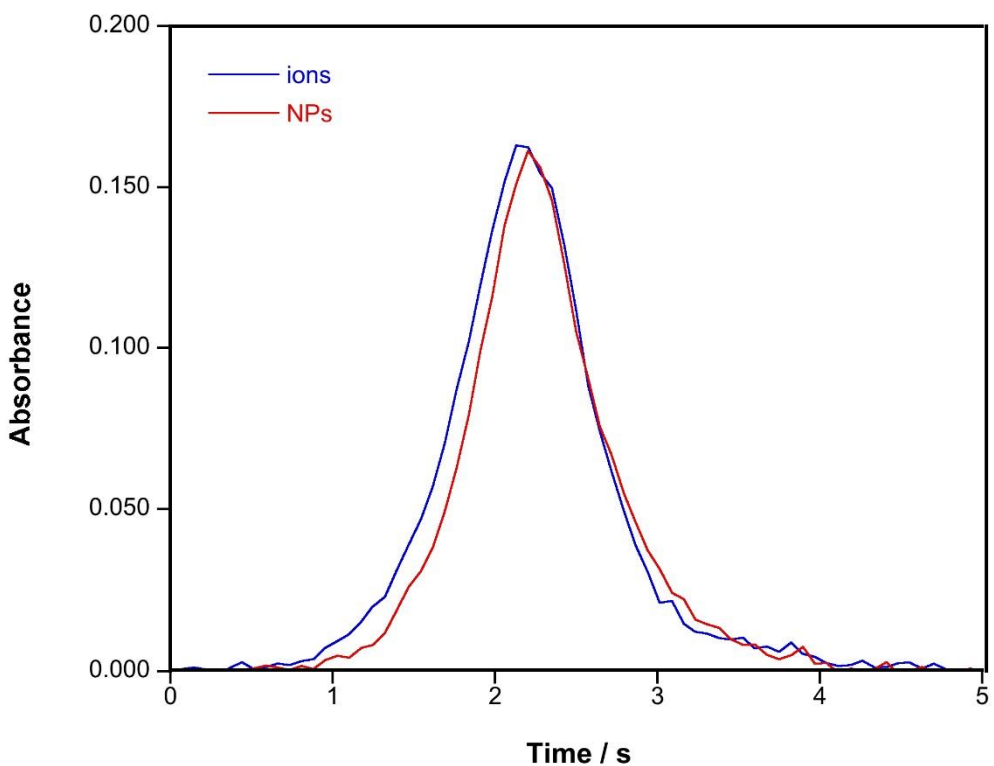


Figura 2: Time-resolved absorbance of ionic Au and AuNPs solutions ($50 \mu\text{g L}^{-1}$) with Pd ($10 \mu\text{g}$) as chemical modifier using standard conditions.

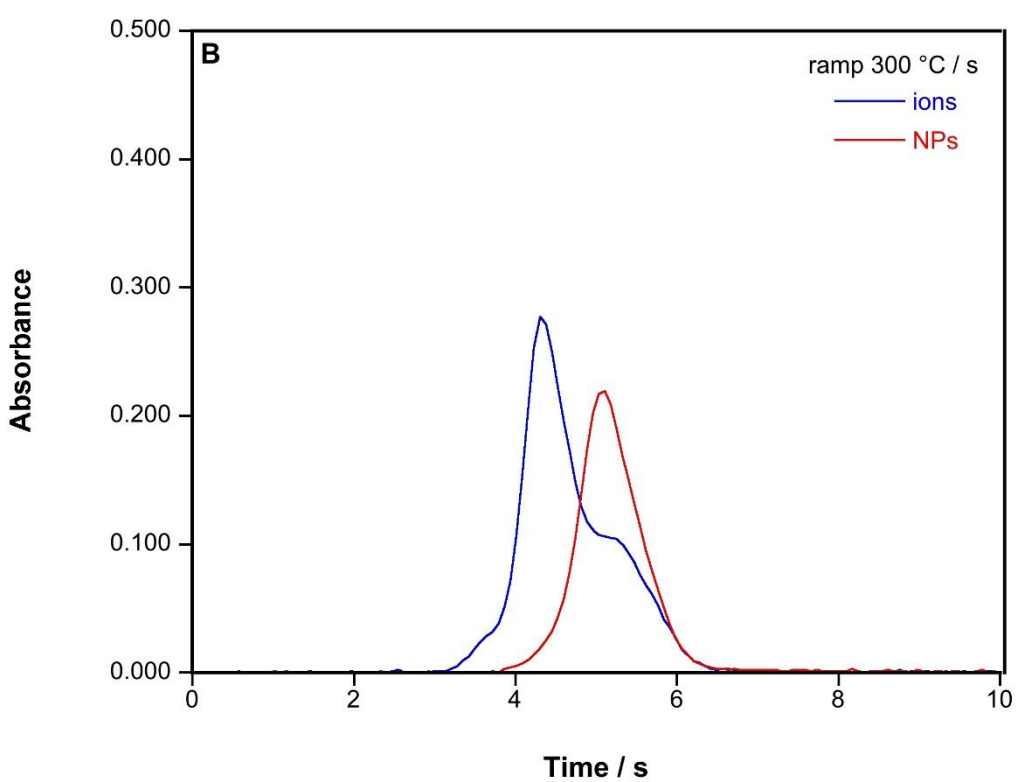
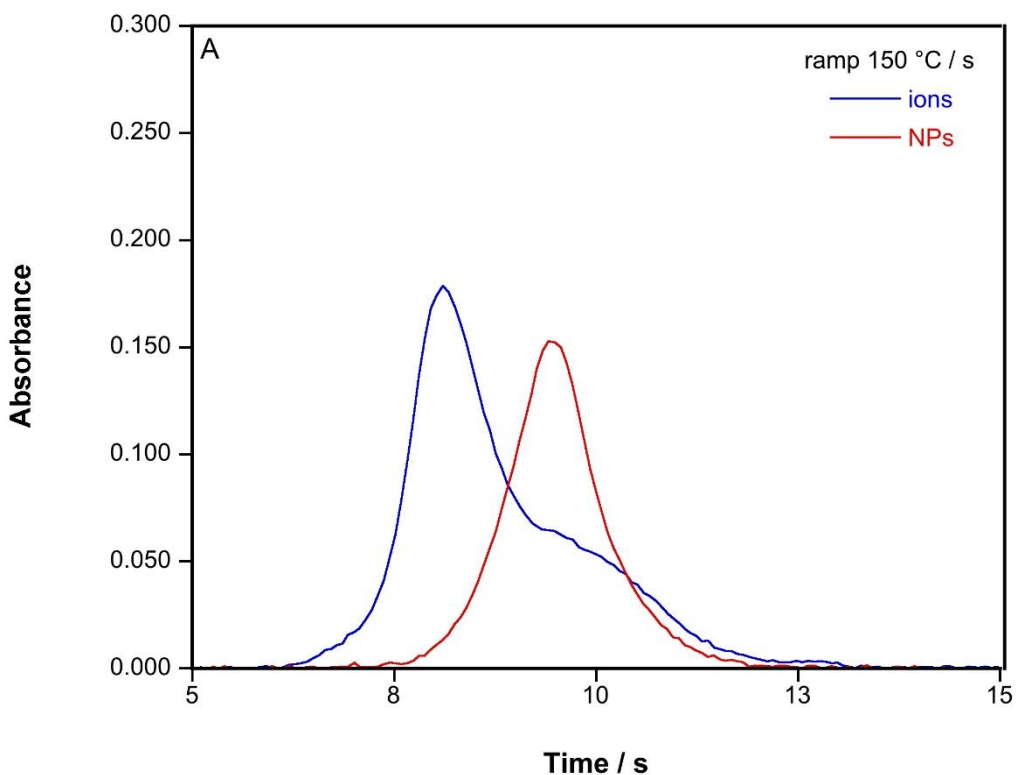
All the conventional methodologies based on the addition of a modifier and fast atomization ramps called stabilized temperature platform furnace (STPF) are against the goal of this work, so, in order to separate ions from NPs, the strategy must be different.

The first article released about differentiating ions and NPs with HR CS GFAAS worked with silver at low atomization temperatures (1700°C). The ionic signal was significantly higher compared with the AgNPs signals and among this the peak is smaller as the size increases.²¹ This means that the atomization process is easier as the species has a smaller size. However, the selectivity was low and the method could not separate between 20 and 60 nm. A more in depth study, carried out by Feitchmeier and Leopold, demonstrated the necessity of optimize other parameters of the temperature program. In contraposition with the previous article, the ionic signal appeared after the NPs signal. The explanation provided by the authors was that the solid matrix was interacting strongly with ions

delaying the signal, proving that every sample behaves differently and must take into account.^{23,24}

With all the previous information, a set of experiments were carried out to separate gold ions and nanoparticles by using HR CS GFAAS. It seems logic to use slow atomization ramps to provide time to maximize the potential differences existing between both atomization mechanisms. This will cause wider and lower signals meaning a worse signal to background ratio, but the higher atomization temperature of Au compared with Ag could improve the differences too

Figure 3 shows the results of two solutions of ionic gold standard and an AuNPs suspension of 50 nm atomized with variable heating ramps. The shape of the ionic Au signals (double peaks) shows an increasing proportion of the second peak as the atomization heating ramp decreases, the shape of the AuNPs signals remains Gaussian independently of the ramp used. These differences in shape as well as the time of the maximum are more notorious for slow atomization heating ramps ($150\text{-}300^{\circ}\text{C s}^{-1}$) up to more than 1 second between maximums. Quantitative results are shown in **table 2**.



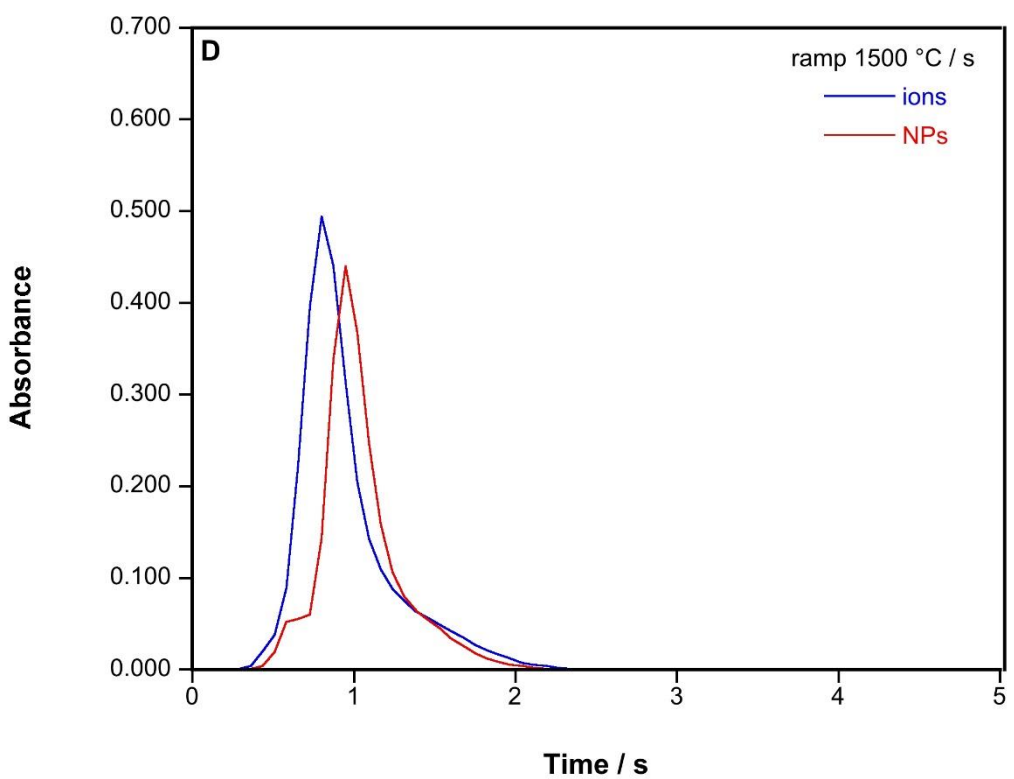
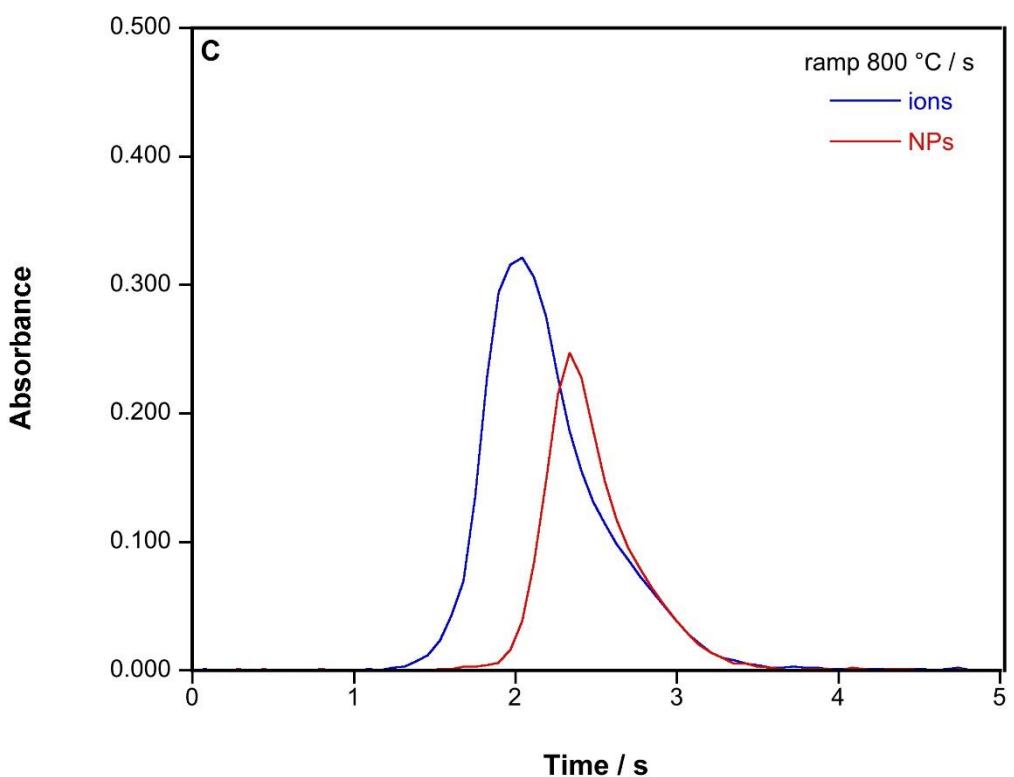


Figure 3: Time-resolved absorbance of ionic Au and AuNPs of 50 nm solutions (70 and 50 $\mu\text{g L}^{-1}$ respectively) with atomization heating ramps of: a) 150°C s^{-1} ; b) 300°C s^{-1} ; c) 800°C s^{-1} and d) $1500^\circ\text{C s}^{-1}$.

Heating ramp / $^\circ\text{C s}^{-1}$	Peak maximum for ionic Au / s	Peak maximum for AuNPs / s	Δt / s	$u_{\Delta t}$ / s
150	8.175	9.489	1.314	0.073
300	4.321	5.073	0.752	0.053
800	1.995	2.287	0.292	0.042
1500	0.817	0.967	0.150	0.049

Table 2: Time of appearance of the maximum peak height for the signals obtained by HR CS GFAAS for solutions containing Au and AuNPs, as a function of the heating ramp applied to the atomization step. Every value is the average of 5 replicates. The uncertainty (u) is expressed as the square root of the sum of the variances of both maximum peak height measurements.

The width of the signals at slow ramps and the double peak of the ionic solutions are the biggest drawbacks of the method, preventing the complete separation of the ionic and the AuNPs and its quantification in mixtures.

This second peak was associated previously to the reduction of gold in the carbon active sites, probably producing NPs of metallic gold of different sizes and precluding the complete separation of signals of different species.

Trying to overcome this problem a set of experiments were carried out. The addition of molecules with S atoms as modifier were added with the intention of favour a stronger interaction between them and the ionic Au and modify its atomization mechanism. The molecules tested were cysteine, thiourea and diluted H_2SO_4 . Unfortunately, the results for these experiments did not improve those obtained previously. Looking for a different

heating profile, the current tube with platform was substituted by another without it. Heating directly from the wall provides a different heating profile, which could derive in a better resolution in the separation. However the results were more irreproducible and the difference in time did not increase.

In conclusion, an atomization ramp of $150\text{ }^{\circ}\text{C s}^{-1}$ with a graphite tube with platform and not adding any chemical modifier was selected as the best method tested.

The next parameter optimized was the atomization temperature as one of the most important to achieve the best resolution possible. Atomization curves of ionic Au and AuNPs of 76 nm showed differences to reach the maximum signal, 1400°C were needed for the ionic Au and 1500°C for the case of the AuNPs.

This difference in the atomization temperature could derive in an improvement in the separation. Thus, a study of sequential atomization temperatures were carried out keeping the selected heating ramp ($150^{\circ}\text{C s}^{-1}$). The samples measured were ionic Au solution and two suspensions of AuNPs (20 and 76 nm). The results for $2000\text{ }^{\circ}\text{C}$ are shown in the **Figure 4** as an example.

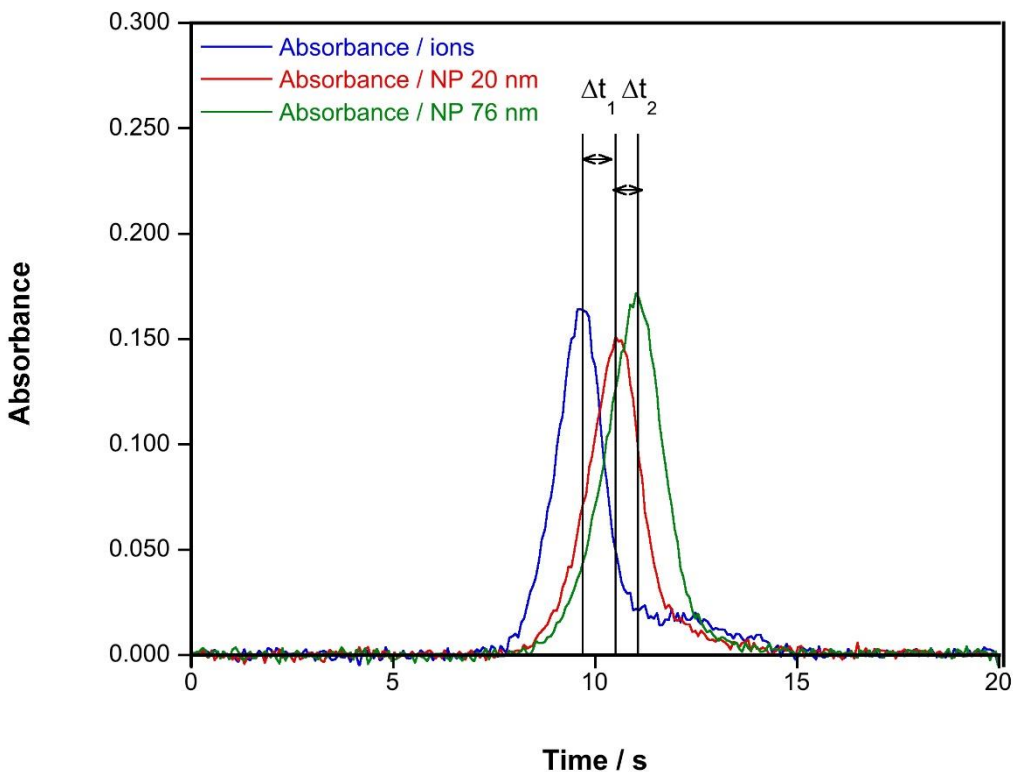


Figure 4: Time-resolved absorbance for an Au aqueous standard ($50 \mu\text{g L}^{-1}$) and for a suspension of AuNPs of 20 and 76 nm in aqueous media ($50 \mu\text{g L}^{-1}$) using an atomization temperature of 2000°C and a heating ramp of $150 \text{ }^\circ\text{C s}^{-1}$

The results exhibit the described double peaks for the ionic Au appearing earlier than the two NPs Gaussian signals which appear in order depending on its size. This sequence dependant on the size could be caused by the necessity of more energy to vaporize higher NPs, but the release of the atoms in the NPs may be faster by the extra energy given to the system contributing the narrowing of the peak, although the size distribution could counteract this effect.

In **table 3** the results of the maximum of the peak at different atomization temperatures are shown, demonstrating that higher temperatures improves the separation, especially between ions and small nanoparticles. However, for bigger nanoparticles the effect is practically nonexistent and an intermediate temperature of 2200°C was selected as the best option to increase the life time of the graphite tube for obtaining good results for small

sized particles and the same resolution compared with 2400°C when the size is increased (20 nm and 76 nm).

Temperature / °C	Δt_1 / s	Δt_2 / s	$u_{\Delta t_1}$ / s	$u_{\Delta t_2}$ / s
2000	0.73	0.44	0.21	0.15
2200	1.17	0.60	0.10	0.13
2400	1.48	0.44	0.16	0.12

Table 3: Time difference of the maximum peak height for the signals obtained by HR CS GFAAS for solutions containing ionic Au and AuNPs (20 and 76 nm), as a function of the atomization temperature.

All the peak areas shown until now were consistent independently of the specie involved, demonstrating the feasibility of this selected parameters to quantify the total amount of Au in the samples analysed.²⁰

In **table 4** are collected all the instrumental parameters used by HR CS GFAAS.

Wavelength	242.795 nm			
Number of detector pixels summed per line	3 (4.20 pm)			
Sample volume	10 μL			
Temperature program				
Step	Temperature / °C s ⁻¹	Ramp / °C s ⁻¹	Hold / s	Ar gas flow / L min ⁻¹
Drying	90	3	20	2.0
Drying	110	5	10	2.0
Pyrolysis	300	50	30	2.0
Pyrolysis	300	0	5	0.0
Atomization	2200	Variable ^a	10	0.0
Cleaning	2450	500	4	2.0

^aA value of 150 °C s⁻¹ was finally selected as optimum.

Table 4: Instrumental parameters used to monitor Au by HR CS GFAAS.

3.2. Evaluation of parameters to characterize the NP size

Along this work, the maximum of the peaks have shown differently depending on the specie (ions appear before NPs) and the size (bigger NPs appear after small NPs). Therefore the time at the maximum of the peak can be treated as a key parameter to determine differences and discriminate between ions and NPs of different sizes. This parameter was already referred by Feichtmeier and Leopold with another that they called atomization rate which is the slope of the upper curve of the peak.²³ Those parameters will be denoted as t_{\max} and k_{at} respectively from now on in this text. To fully characterize the signal another parameter was evaluated, the peak width at 50% of the maximum absorbance, denoted as $\Delta t_{1/2}$. To calculate k_{at} the first part of the peaks were adjusted linearly around the first inflection point with at least $R^2 > 0.9$ and a minimum of 50 points. A scheme of this three parameters can be seen in **figure 5**.

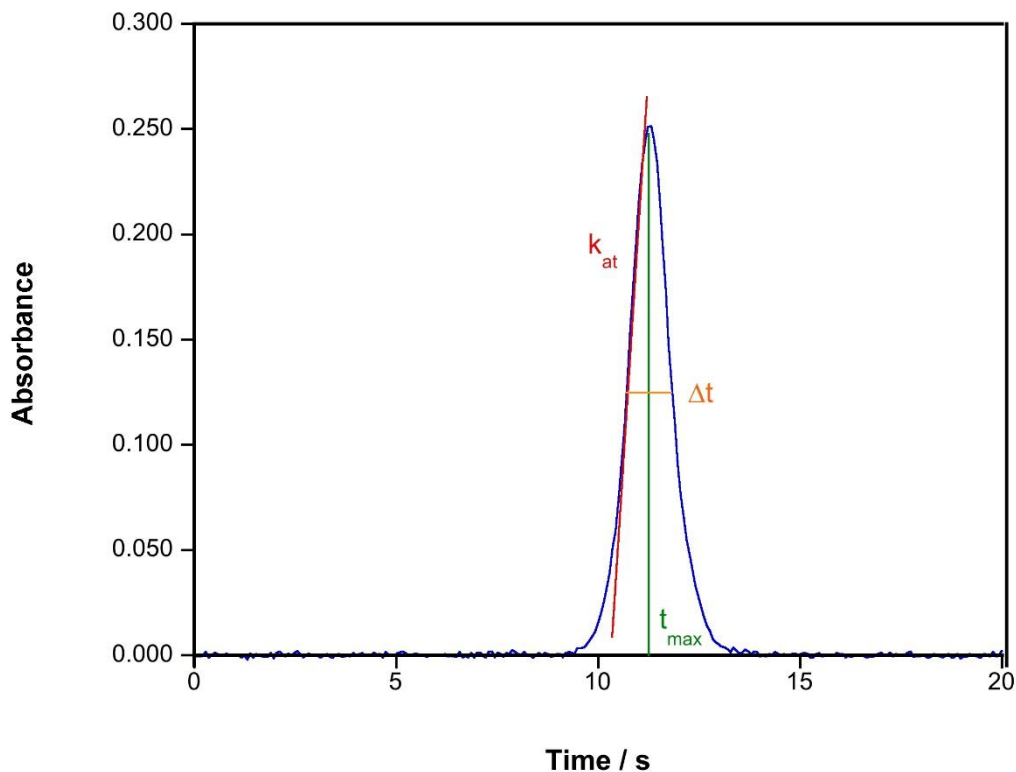
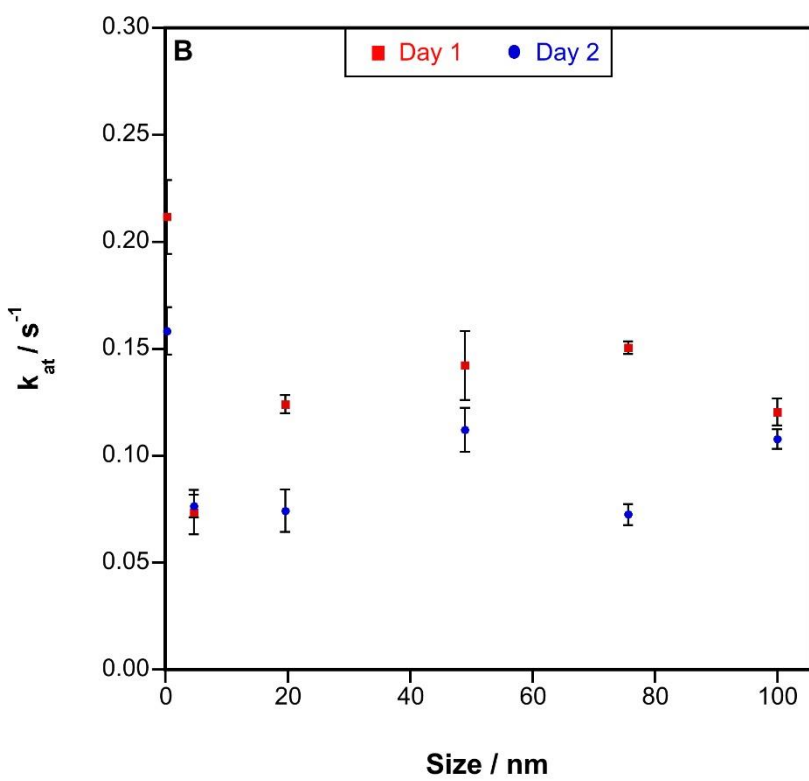
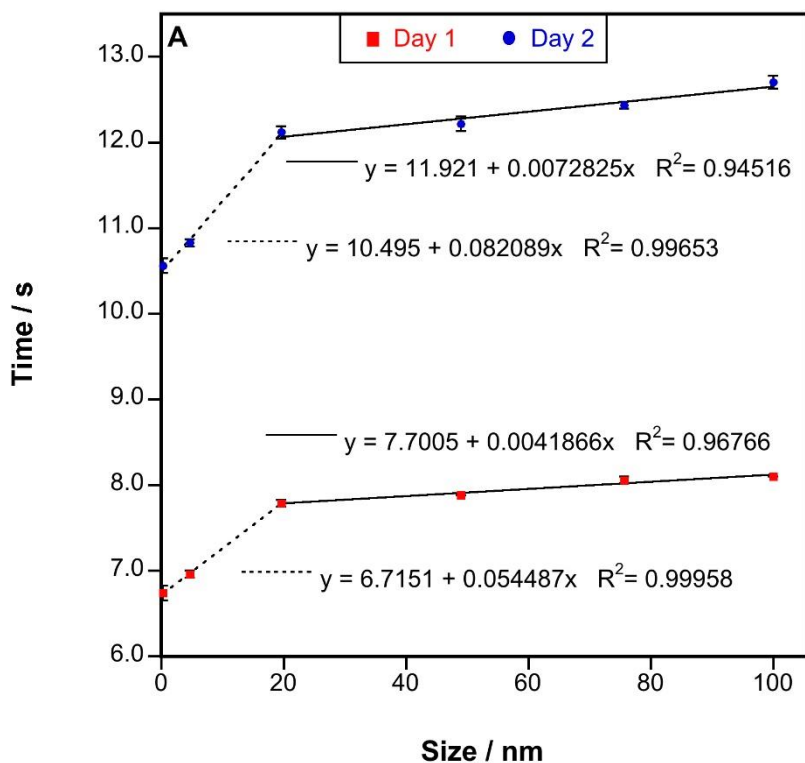


Figure 5: Example of a time-resolved absorbance signal obtained for a suspension of AuNPs (76 nm) in aqueous media showing the different parameters evaluated in this work.

The results obtained after evaluate this three parameters are collected in **figure 6**, comparing the results of two different days to evaluate the reproducibility of the parameters chosen. **Figure 6a** shows the values of t_{\max} versus size, for ions the ionic diameter of Au was selected. It is clear that this first parameter depends on the size of the particle and can be correlated linearly in two regions, the first region from ions to 20 nm, with a bigger slope, indicating a better resolution and a second region from 20 to 100 nm with a softer slope, decreasing the differences while the size is increased. The resolution for other techniques worsen while the size of the NPs decrease, being a potential alternative for small NPs.^{6,15}

Comparing the results of both days, it can be seen the necessity of calibrate every day. The region of appearance of the signals and the sensitivity varies and it has been seen the influence of the age of the graphite tube, delaying the signals as the tube is wearing away. Therefore, a calibration at the start of a new day would be needed with at least three points: Ionic Au, 20 nm and 76 or 100 nm to define the two linear ranges.

The other two parameters (**figures 6b and 6c**) did not show such clear and direct tendency as the t_{\max} . The atomization rate, k_{at} , seems to have a certain tendency increasing with the NPs size, but the uncertainty makes this parameter unacceptable and hardly interpretable. (14% DSR). The value for ionic Au, bigger than for any NPs measured, makes this parameter useless for the characterization of ions. In addition, a correlation with the concentration were observed and will be described later. Finally, the last parameter ($\Delta t_{1/2}$) showed no tendencies and is related with the concentration as the previous parameter.



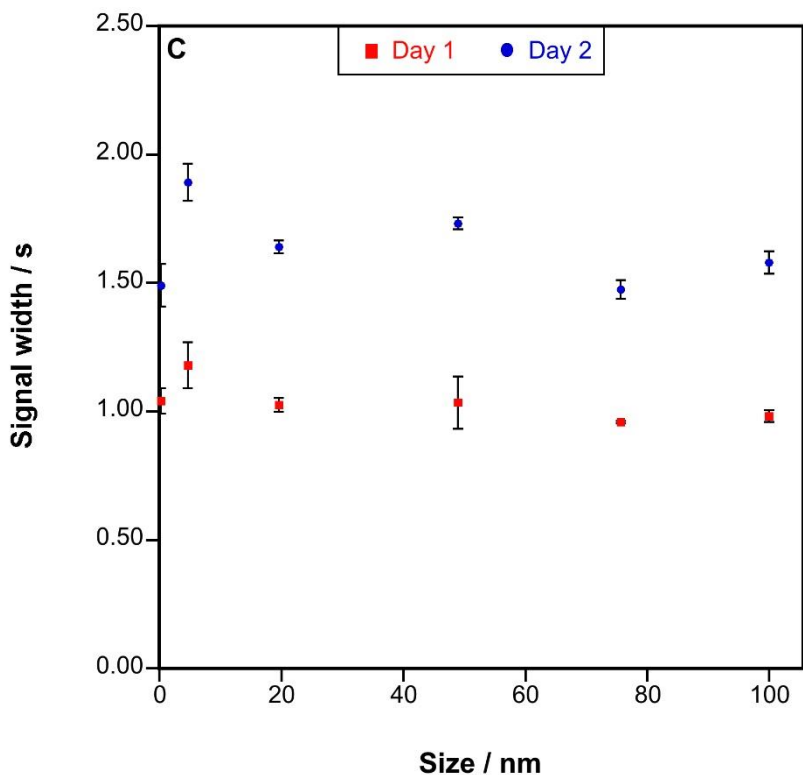


Figure 6: Representation of signal parameters compared with AuNPs size: a) t_{\max} ; b) k_{at} ; c) $\Delta t_{1/2}$. Results of two different days are shown with their uncertainties calculated with 5 replicates.

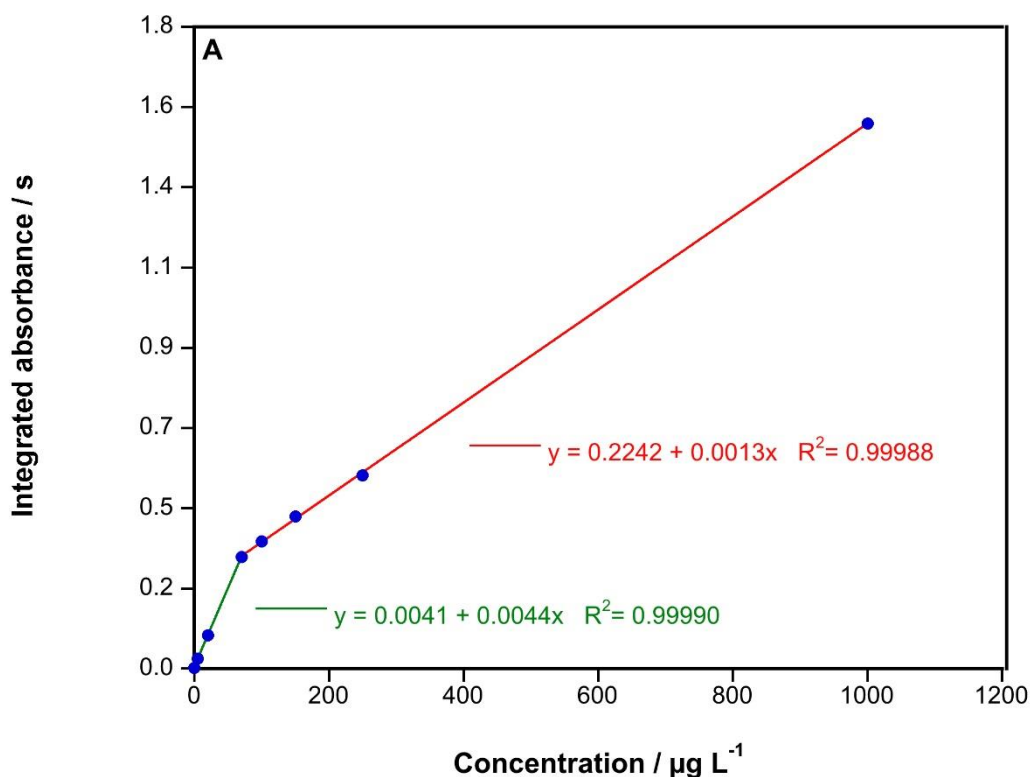
Summarizing, only the time at the maximum of the peak accomplished the requirements to characterize the size of the AuNPs. The method was also evaluated by interpolating a sample from another manufacturer (NIST) obtaining a result of 27.7 ± 8.8 nm fitting perfectly with the result provided (27.6 ± 2.1 nm measured by TEM).

3.3. Analytical performance

With a suspension of AuNPs of 76 nm, different analytical parameters were evaluated. The limit of detection (LOD) calculated as three times the standard deviation of ten blank replicates divided by the slope of the calibration curve, gives a result of 5.5 pg, demonstrating the capability of the method to perform trace analysis.

The next parameter studied was the linearity of the method, and as can be seen in **figure 7a**, two linear regions clearly defined appear, the first region covers the LOD up to $70 \mu\text{g L}^{-1}$, and the second last from 70 to $1000 \mu\text{g L}^{-1}$. This behaviour was already observed for other elements using this technique.²⁹ Therefore, quantification of Au can cover around three orders of magnitude in this conditions.

Figure 7b shows signals of AuNPs of 76 nm at different concentrations, demonstrating that t_{\max} is a parameter independent of the amount of the element introduced in the tube and establishing as the key parameter to determine the size of the NPs without the necessity of compare solutions of the same range of concentration. It also can be seen how the other two parameters studied (k_{at} and $\Delta t_{1/2}$) has a strong influence with the concentration, making this parameters useless unless the concentration of the suspensions were equal.



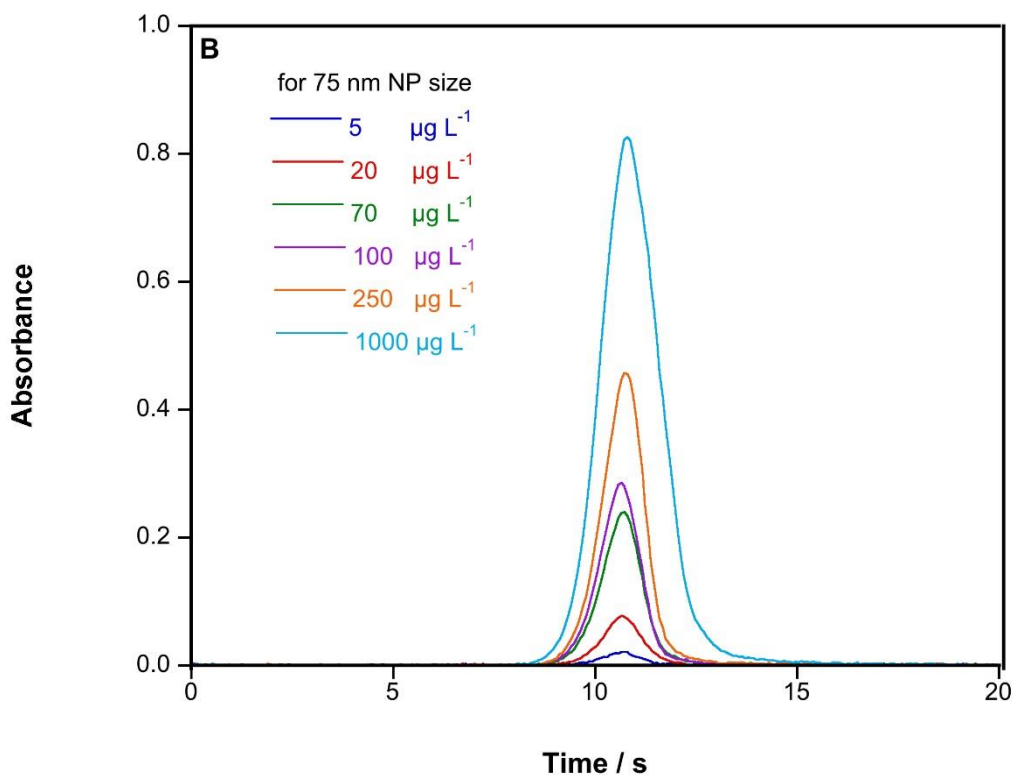


Figure 7: a) Linearity observed measuring AuNPs of 76 nm aqueous standard of different concentrations. b) Time-resolved signals for an AuNPs of 76 nm aqueous standard of different concentrations.

The method was evaluated in a real sample to test the possible matrix effects. The sample used was a certified reference material from the Kejimkujik Lake in Canada (KEJIM 02), a soft water containing several ions and carbon matter at the mg L^{-1} range that could interact with Au. The sample was spiked with $50 \mu\text{g L}^{-1}$ of ionic Au and AuNPs of 5, 20, 50, 75 and 100 nm and evaluated the parameters determined in section 3.2 (t_{\max} , k_{at} and $\Delta t_{1/2}$) and under the conditions optimized previously (table 4). The results of **figure 8** shows how the tendencies of the three parameters remains the same, showing an increment in the t_{\max} with the size of the particle with a change in the slope at 20 nm. The results obtained from the other two parameters showed the same trend than in the aqueous suspensions.

Summarizing, no matrix effect was found when the method is evaluated in an environmental soft water sample, demonstrating its feasibility for this type of samples.

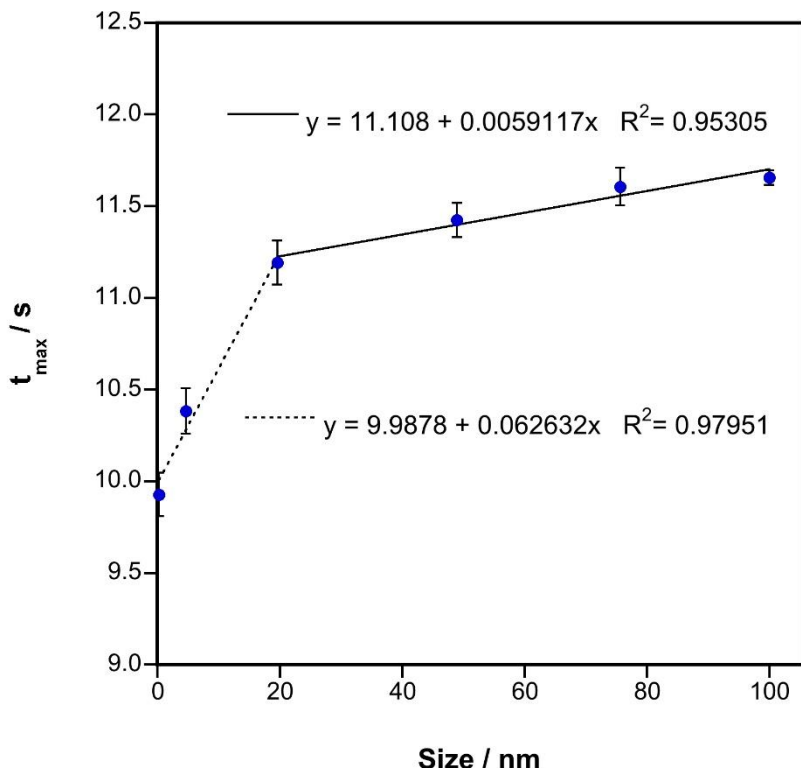


Figure 8: Representation of t_{\max} compared with AuNPs size for KEJIM-02 solutions/suspensions spiked with $70 \mu\text{g L}^{-1}$ of ionic Au and AuNPs. Uncertainties calculated with 5 replicates.

Finally, the possibility of elucidate the presence of ions and NPs in mixtures was studied. Three different aqueous solutions were prepared with ionic Au, AuNPs of 76 nm and the last with both species of Au with the same concentration. The profile of the signal have been already discussed, being able to differentiate them just by visual inspection (shape) and also by the t_{\max} parameter, but when a mixture of ions and nanoparticles is measured, a double signal is clearly found, being the second peak more pronounced due to the contribution of the AuNPs and the second peak of the ionic Au associated to part of this Au atomized by a reduction mechanism via carbon active sites. The sum of the areas and the shape of the two signals of ionic Au and AuNPs separately provides a similar result as the area calculated for the signal measured with the mixture as can be seen in **figure 9**.

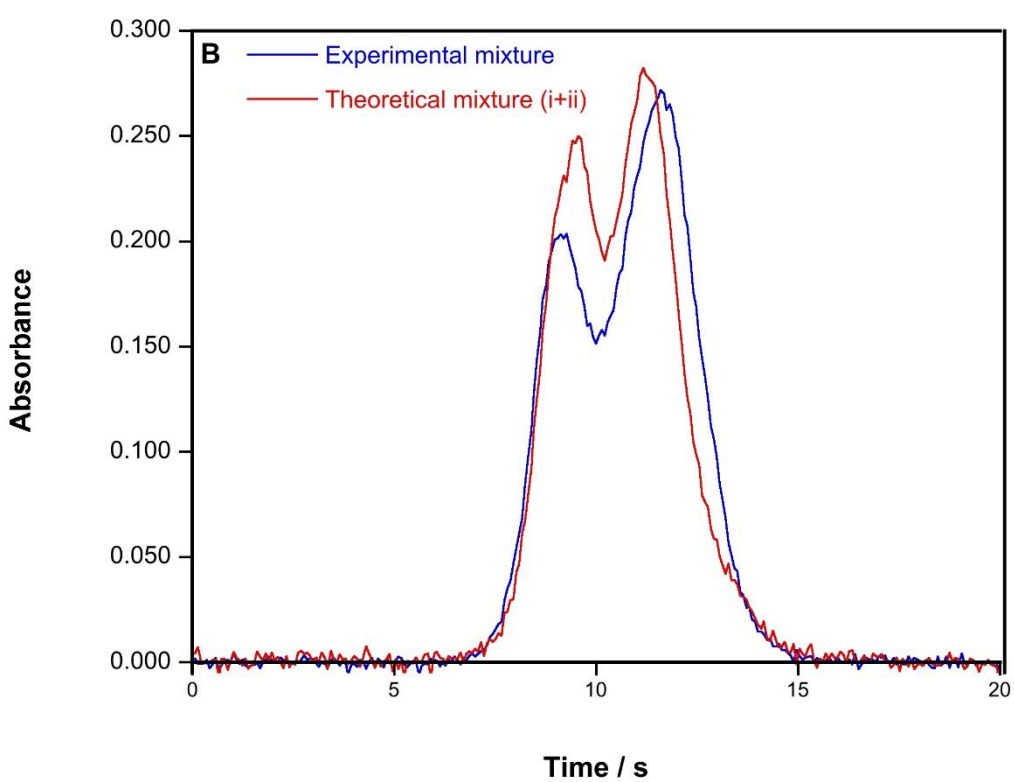
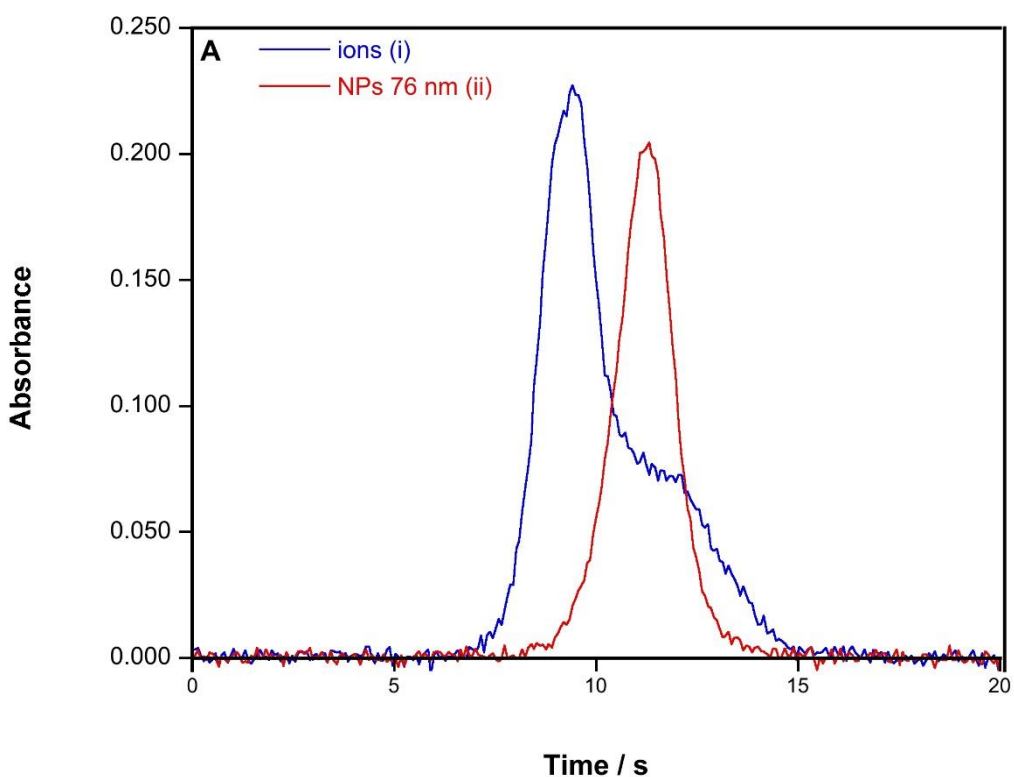


Figure 9: Time-resolved absorbance for: a) an Au aqueous standard (i) and an aqueous suspension of AuNPs of 76 nm (ii); b) Mixture of both ionic Au and AuNPs of 76 nm experimentally obtained and calculated as the sum of signals from figure 9a.

4. Conclusions

The application of slow atomization ramps and the absence of modifiers allow to HR CS GFAAS to obtain analytical information to differentiate between ionic and nanoparticles of Au in aqueous solutions in a fast and simple way.

It has been demonstrated that the time of appearance of the maximum of the peak can be related with the particle size, due to the delay caused by the difficulty to atomize bigger particles. This parameter follows a trend that can be measured and exploited for the calculation of the size of uncharacterized AuNPs with a calibration curve, a few requirements and keeping the quantitative information provided by the technique.

The linear range of the method provides information for at least three orders of magnitude with a LOD of 5.5 pg. Only the time at the maximum of the signal remains stable independently from the concentration, therefore is the only parameter suitable for the characterization of the size of the AuNPs in aqueous solutions. The evaluation of the method in an environmental sample (KEJIM-02) demonstrates the feasibility of the method in the presence of ions such as sulfates, chlorides and carbon matter.

Mixtures of ions and NPs of Au can be detected but not quantified, however, with the introduction of a previous separation step the analysis by GFAAS seems to be perfectly suitable.³⁰⁻³²

The possibility to make direct analyses in solid samples in conjunction with the results obtained makes this technique a promising approach for the future.

5. Bibliography

1. T.L. Doane and C. Burda, *Chem. Soc. Rev.*, 2012, **41**, 2885–2911.
2. R.R. Arvizo, S. Bhattacharyya, R.A. Kudgus, K. Giri, R. Bhattacharya and P. Mukherjee, *Chem. Soc. Rev.*, 2012, **41**, 2943–2970.
3. Y. Ju-Nam and J.R. Lead, *Sci. Total Environ.*, 2008, **400**, 396–414.
4. E.C. Dreden, A.M. Alkilany, X. Huang, C.J. Murphy and M.A. El-Sayed, *Chem. Soc. Rev.*, 2012, **41**, 2740–2779.
5. K.L. Aillon, Y. Xie, N. El-Gendy, C.J. Berkland and M.L. Forrest, *Adv. Drug Deliv. Rev.*, 2009, **61**, 457–466.
6. S. Lee, X. Bi, R.B. Reed, J.F. Ranville, P. Herckes and P. Westerhoff, *Environ. Sci. Technol.*, 2014, **48**, 10291–10300.
7. S. Barlow, A. Chesson, J.D. Collins, A. Flynn, A. Hardy, K.D. Jany, A. Knaap, H. Kuiper, J.C. Larsen, P. Le Neindre, J. Schans, J. Schlatter, V. Silano, S. Skerfving and P. Vannier, *The EFSA Journal*, 2009, **958**, 1–39.
8. P.-C. Lin, S. Lin, P. C. Wang, R. Sridhar. *Biotechnology Advances.*, 2014, **32**, 711-726.
9. L. Yu and A. Andriola, *Talanta*, 2010, **82**, 869–875.
10. S. Bhattacharjee. *Journal of Controlled Release*, 2016, **235**, 337-351.
11. P. Krystek, A. Ulrich, C.C. Garcia, S. Manohar and R. Ritsema, *J. Anal. At. Spectrom.*, 2011, **26**, 1701–1721.
12. P. Krystek, *Microchem. J.*, 2012, **105**, 39–43.
13. A.R. Montoro Bustos, J.R. Encinar and A. Sanz-Medel, *Anal. Bioanal. Chem.*, 2013, **405**, 5637–5643.
14. C. Degueldre, P.Y. Favarger and S. Wold, *Anal. Chim. Acta*, 2006, **555**, 263–268.
15. J. Liu, K.E. Murphy, R.I. MacCuspie and M.R. Winchester, *Anal. Chem.*, 2014, **86**, 3405–3414.
16. R. Peters, Z. Herrera-Rivera, A. Undas, M. van der Lee, H. Marvin, H. Bouwmeester and S. Weigel, *J. Anal. At. Spectrom.*, 2015, **30**, 1274– 1285.
17. B. Meermann and F. Laborda, *J. Anal. At. Spectrom.*, 2015, **30**, 1226– 1228.
18. G.M. Fent, S.W. Casteel, D.Y. Kim, R. Kannan, K. Katti, N. Chanda and K. Katti, *Nanomedicine*, 2009, **5**, 128–135.

19. M. Resano, M. Aramendía and M.A. Belarra, *J. Anal. At. Spectrom.*, 2014, **29**, 2229–2250.
20. M. Resano, E. Mozas, C. Crespo, J. Briceño, J. del Campo-Menoyo and M. A. Belarra, *J. Anal. At. Spectrom.*, 2010, **25**, 1864–1873.
21. M. Resano, A.C. Lapeña and M.A. Belarra, *Anal. Methods*, 2013, **5**, 1130–1139.
22. F. Gagné, P. Turcotte and C. Gagnon, *Anal. Bioanal. Chem.*, 2012, **404**, 2067–2072.
23. N.S. Feichtmeier and K. Leopold, *Anal. Bioanal. Chem.*, 2014, **406**, 3887–3894.
24. N.S. Feichtmeier, N. Ruchter, S. Zimmermann, B. Sures and K. Leopold, *Anal. Bioanal. Chem.*, 2016, **408**, 295–305.
25. B. Welz, H. Becker-Ross, S. Florek and U. Heitmann, *High-Resolution Continuum Source AAS. The better way to do atomic absorption spectrometry*, Wiley-VCH, Weinheim, 2005.
26. M. Resano, M. Aramendía, E. Garcia-Ruiz and M. Belarra, *J. Anal. At. Spectrom.*, 2005, **20**, 479–481.
27. E. Iwamoto, M. Itamoto, K. Nishioka, S. Imai, Y. Hayashi and T. Kumamaru, *J. Anal. At. Spectrom.*, 1997, **12**, 1293–1296.
28. N. S. Thomaidis and E. A. Piperaki and C. E. Efstathiou, *Spectrochim. Acta Part B*, 1999, **54**, 1303–1320.
29. B. Welz, L.M.G. dos Santos, R.G.O. Araujo, S. do C. Jacob, M.G.R. Vale, M. Okruss and H. Becker-Ross, *Spectrochim Acta B*, 2010, **65**, 258–262.
30. G. Hartmann and M. Schuster, *Anal. Chim. Acta*, 2013, **761**, 27–33.
31. I. López-García, Y. Vicente-Martínez and M. Hernández-Córdoba, *Spectrochim. Acta Part B*, 2014, **101**, 93–97.
32. K. Leopold, A. Philippe, K. Wörle and G.E. Schaumann, *Trends. Anal. Chem.*, 2016, in press, doi: 10.1016/j.trac.2016.03.026.